



# Hindered magnetic dipole transitions between $P$ -wave bottomonia and coupled-channel effects

Feng-Kun Guo<sup>a</sup>, Ulf-G. Meißner<sup>a,b,c</sup>, Zhi Yang<sup>a,b,\*</sup>

<sup>a</sup> CAS Key Laboratory of Theoretical Physics, Institute of Theoretical Physics, Chinese Academy of Sciences, Beijing 100190, China

<sup>b</sup> Helmholtz-Institut für Strahlen- und Kernphysik and Bethe Center for Theoretical Physics, Universität Bonn, D-53115 Bonn, Germany

<sup>c</sup> Institut für Kernphysik, Institute for Advanced Simulation and Jülich Center for Hadron Physics, Forschungszentrum Jülich, D-52425 Jülich, Germany

## ARTICLE INFO

### Article history:

Received 12 April 2016

Received in revised form 17 June 2016

Accepted 7 July 2016

Available online 14 July 2016

Editor: B. Grinstein

## ABSTRACT

In the hindered magnetic dipole transitions of heavy quarkonia, the coupled-channel effects originating from the coupling of quarkonia to a pair of heavy and anti-heavy mesons can play a dominant role. Here, we study the hindered magnetic dipole transitions between two  $P$ -wave bottomonia,  $\chi_b(nP)$  and  $h_b(n'P)$ , with  $n \neq n'$ . In these processes the coupled-channel effects are expected to lead to partial widths much larger than the quark model predictions. We estimate these partial widths which, however, are very sensitive to unknown coupling constants related to the vertices  $\chi_{b0}(nP)B\bar{B}$ . A measurement of the hindered M1 transitions can shed light on the coupled-channel dynamics in these transitions and hence on the size of the coupling constants. We also suggest to check the coupled-channel effects by comparing results from quenched and fully dynamical lattice QCD calculations.

© 2016 Published by Elsevier B.V. This is an open access article under the CC BY license (<http://creativecommons.org/licenses/by/4.0/>). Funded by SCOAP<sup>3</sup>.

In recent years, several new bottomonia were discovered. One of the most interesting discoveries is the  $h_b(1P)$  found in the puzzling  $\pi^0$  transition  $\Upsilon(3S) \rightarrow \pi^0 h_b(1P)$  with a subsequent electric dipole (E1) transition to the  $\eta_b(1S)$  by the Babar collaboration [1]. This finding is consistent with the prediction that such a transition is a promising way to produce the  $h_b$  [2,3]. The isospin violating decay channel has the same final states,  $\gamma\gamma h_b$ , as the one in the electromagnetic cascades  $\Upsilon(3S) \rightarrow \gamma\chi_{bJ}(2P)$  ( $J = 0, 1, 2$ ) and  $\chi_{bJ}(2P) \rightarrow \gamma h_b$ . The branching fractions for the E1 transitions  $\Upsilon(3S) \rightarrow \gamma\chi_{bJ}(2P)$  are well measured to be of the order of 10%, but no experimental result for the hindered magnetic dipole (M1) transition  $\chi_{bJ}(2P) \rightarrow \gamma h_b$  is available. Thus, it is important to investigate the decay channel  $\chi_{bJ}(2P) \rightarrow \gamma h_b$ . The  $h_b(1P)$  later on was also observed in the isospin conserving decay process  $\Upsilon(4S) \rightarrow \eta h_b$  [4] with a branching fraction  $(2.18 \pm 0.21) \times 10^{-3}$ , consistent with the estimate of the order  $10^{-3}$  in Ref. [5], where this channel was suggested to be used to search for the  $h_b$ .

The quark model has been used to study the spectrum and decay properties of the excited bottomonia without the coupled-channel effects from intermediate open-bottom mesons [6]. The spectrum was also calculated with the inclusion of coupled-

channel effects [7]. More generally, we remark that coupled-channel effects due the virtual hadronic loops are of recent interest in heavy quarkonium physics. In the quenched quark model, the mixture between the bare hadron states and the two-meson continuum is not taken into account. When the coupled-channel effects are considered, the quarkonium spectrum gets shifted (the values of these mass shifts depend on the specific models, see, e.g., Refs. [7–16]). In addition to the impact on the mass spectrum, the coupled-channel effects are expected to be important in some transitions between heavy quarkonia [17–27]. In particular, they are expected to dominate the hindered M1 transitions between the  $P$ -wave quarkonia because of two reasons: first, the hindered M1 transitions break heavy quark spin symmetry and their widths in the quark model come from relativistic corrections; second, the coupled-channel contribution has an enhancement due to the  $S$ -wave couplings of the two vertices involving heavy quarkonia [28]. For instance, the partial width of  $\chi_{c2}(2P) \rightarrow \gamma h_c(1P)$  from the coupled-channel effects is two orders of magnitude larger than the prediction from the quark model as shown in Ref. [28]. Such hindered M1 transitions between bottomonia may be measured at Belle-II [29]. However, although there have been calculations on hindered M1 transitions between  $S$ -wave heavy quarkonia in the framework of effective field theory [30,31] and lattice QCD [32–35], so far only a few predictions on similar transitions between  $P$ -wave bottomonia have been given, and all of them are based on quark model calculations [6]. Since in bottomonium

\* Corresponding author.

E-mail addresses: [fkguo@itp.ac.cn](mailto:fkguo@itp.ac.cn) (F.-K. Guo), [meissner@hiskp.uni-bonn.de](mailto:meissner@hiskp.uni-bonn.de) (U.-G. Meißner), [zhiyang@hiskp.uni-bonn.de](mailto:zhiyang@hiskp.uni-bonn.de) (Z. Yang).

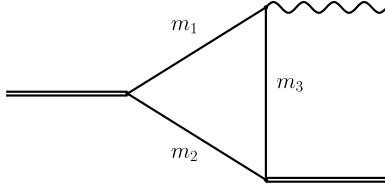


**Fig. 1.** Triangle diagram where the double, solid and wavy lines represent the bottomonium, bottomed meson and the photon, respectively.

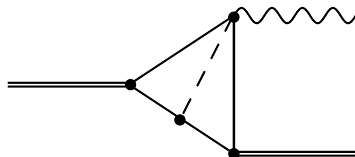
systems the relativistic corrections are small, the quark model predictions on these partial widths are tiny, in the range from sub-eV to eV. Yet, similarly to the charmonia case, the coupled-channel effects due to virtual bottom mesons could enhance the decay widths to values that make an observation possible. This motivates us to study here the hindered M1 transitions between  $P$ -wave bottomonia by considering the coupled-channel effects through coupling to virtual bottom and anti-bottom mesons. An additional important motivation for us to study these processes is the fact that experimentalists plan to study them at the coming Belle-II experiment [29].

Due to the fact that the bottomonia are close to the open bottom thresholds so that the intermediate bottom mesons are non-relativistic, we use nonrelativistic effective field theory (NREFT) suitable for investigating such coupled-channel effects in heavy quarkonia transitions [23,24,36]. The intermediate mesons are non-relativistic so that their velocities, denoted by  $v$ , are much smaller than one, and the loop diagrams scale in powers of  $v$ . The three-momentum and kinetic energy are counted as  $v$  and  $v^2$ , respectively, and each of the nonrelativistic propagators scales as  $v^{-2}$ . Further, a  $P$ -wave bottomonium couples to a pair of ground state bottom and anti-bottom mesons in an  $S$ -wave. At leading order, the coupling is described by a constant which does not contribute any power to the velocity counting. Thus, the triangle diagram in Fig. 1 scales as [28]

$$\mathcal{A}_{\text{triangle}} \propto \frac{v^5}{(v^2)^3} \frac{E_\gamma}{m_b} = \frac{E_\gamma}{vm_b}, \quad (1)$$

where the factors  $1/m_b$  and  $E_\gamma$  are due to the spin-flip of the heavy quark in M1 transitions and the  $P$ -wave coupling of the photon to the bottom mesons, respectively. One thus sees that the closer the bottomonia to the bottom-meson thresholds, the larger the coupled-channel effects. One remark is in order:  $v$  in the power counting is in fact the average of two velocities. This can be estimated as  $v = (v_i + v_f)/2$  with  $v_i = \sqrt{|m_1 + m_2 - M_i|/\bar{m}_{12}}$  and  $v_f = \sqrt{|m_2 + m_3 - M_f|/\bar{m}_{23}}$ , where  $m_{1,2,3}$  are the masses of intermediate mesons as labeled in Fig. 1,  $M_{i(f)}$  is the mass for the initial (final) bottomonium, and  $\bar{m}_{jk}$  is the averaged value of  $m_j$  and  $m_k$ .

However, unlike the case of charmonium hindered M1 transitions, the two-loop diagrams with a pion exchanged between two intermediate bottom mesons are not highly suppressed for the bottomonium transitions. From the power counting analysis in Ref. [28], the relative importance of the two-loop diagrams shown in Fig. 2 in comparison with the triangle diagram given in Fig. 1 can be described by a factor



$$\frac{\mathcal{A}_{2\text{-loop}}}{\mathcal{A}_{\text{triangle}}} \sim v \frac{g^2 M_B^2}{\Lambda_\chi^2}, \quad (2)$$

where  $M_B$  is the bottom meson mass,  $\Lambda_\chi = 4\pi F_\pi$ , with  $F_\pi$  the pion decay constant, is the chiral symmetry breaking scale, and  $g \simeq 0.5$  is the axial coupling constant for bottom mesons [37–39]. This ratio can be understood as follows (taking the left diagram in Fig. 2 as an example): the two more propagators and one more nonrelativistic loop integral measure, in comparison with the diagram in Fig. 1, together give the factor  $v = v^5/(v^2)^2$  in the above equation;  $g^2/\Lambda_\chi^2$  comes from the two pionic vertices and one more loop;  $M_B^2$  is introduced to make the ratio dimensionless. Taking the masses of the  $1P$ ,  $2P$  and  $3P$  bottomonia from Refs. [40, 41], the velocity in the power counting may be estimated to be 0.31, 0.23 and 0.18 for the  $2P \rightarrow 1P$ ,  $3P \rightarrow 1P$  and  $3P \rightarrow 2P$  radiative transitions, respectively. One then finds that the relative factor given in Eq. (2) is of order one, which means that the contribution of two-loop diagrams like the ones shown in Fig. 2 should be of similar size as the one-loop triangle diagram in Fig. 1. This is different from the charmonium case studied in Ref. [28] where  $M_B^2$  is replaced by the much smaller  $M_D^2$  and thus leads to a suppression. Nevertheless, we will only calculate the triangle diagram, and keep in mind that given the power counting of the two-loop diagrams such a calculation can only be regarded as an estimate, rather than a precise calculation, with a quantitative uncertainty analysis out of reach.

As a result of the approximate heavy quark spin symmetry, one can classify the heavy-light bottom mesons according to the total angular momentum of the light degrees of freedom  $s_\ell$  and collect them in doublets with total spin  $J = s_\ell \pm \frac{1}{2}$ . For instance, the pseudoscalar ( $P_a$ ) and vector ( $V_a$ ) bottom mesons are collected in the spin multiplet with  $s_\ell^P = \frac{1}{2}^-$ . The two-component effective fields [42] that describe the ground state heavy mesons in the heavy quark limit are  $H_a = \bar{V}_a \cdot \vec{\sigma} + P_a$  for annihilating bottom mesons and  $\bar{H}_a = -\bar{V}_a \cdot \vec{\sigma} + \bar{P}_a$  for annihilating anti-bottom mesons, where  $\vec{\sigma}$  are the Pauli matrices and  $a$  is the light flavor index. Moreover, the  $P$ -wave bottomonia can be collected in a spin multiplet as

$$\chi^i = \sigma^j \left( -\chi_{b2}^{ij} - \frac{1}{\sqrt{2}} \epsilon^{ijk} \chi_{b1}^k + \frac{1}{\sqrt{3}} \delta^{ij} \chi_{b0} \right) + h_b^i. \quad (3)$$

As mentioned above, the leading order coupling of the  $P$ -wave bottomonium to the bottom and anti-bottom mesons is in an  $S$ -wave, and thus is given by [36,43]

$$\mathcal{L}_\chi = i \frac{g_1}{2} \text{Tr}[\chi^\dagger H_a \sigma^i \bar{H}_a] + h.c., \quad (4)$$

where  $\text{Tr}$  denotes the trace in the spinor space. We also need the magnetic coupling of the photon to the  $S$ -wave heavy mesons [26, 42,44]

$$\mathcal{L}_\gamma = \frac{e\beta}{2} \text{Tr}[H_a^\dagger H_b \vec{\sigma} \cdot \vec{B} Q_{ab}] + \frac{eQ'}{2m_Q} \text{Tr}[H_a^\dagger \vec{\sigma} \cdot \vec{B} H_a], \quad (5)$$

where  $B^k = \epsilon^{ijk} \partial^j A^k$  is the magnetic field,  $Q_{ab} = \text{diag}(2/3, -1/3, -1/3)$  is the light quark electric charge matrix,  $Q'$  is the heavy

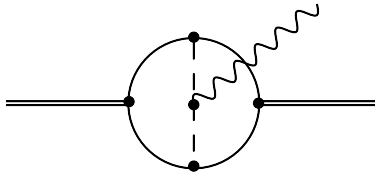


**Fig. 2.** Two typical two-loop diagrams where the double, solid and wavy lines are the same as in Fig. 1 and the dashed lines represent the exchanged pions.

**Table 1**

Triangle loops contributing to each transition, where the mesons are listed as  $[m_1, m_2, m_3]$  corresponding to the notations in Fig. 1. For simplicity, the charge conjugation modes and the light flavor labels are not shown here.

$\chi_{b0} \rightarrow h_b \gamma$	$[B^*, \bar{B}^*, B], [B^*, \bar{B}^*, B^*], [B, \bar{B}, B^*]$
$\chi_{b1} \rightarrow h_b \gamma$	$[B^*, \bar{B}, B^*], [B, \bar{B}^*, B^*]$
$\chi_{b2} \rightarrow h_b \gamma$	$[B^*, \bar{B}^*, B], [B^*, \bar{B}^*, B^*]$
$h_b \rightarrow \chi_{b0} \gamma$	$[B^*, \bar{B}, B], [B, \bar{B}^*, B^*], [B^*, \bar{B}^*, B^*]$
$h_b \rightarrow \chi_{b1} \gamma$	$[B^*, \bar{B}, B^*], [B^*, \bar{B}^*, B]$
$h_b \rightarrow \chi_{b2} \gamma$	$[B, \bar{B}^*, B^*], [B^*, \bar{B}^*, B^*]$

**Table 2**

Decay widths for the hindered M1 transitions between  $\chi_{bJ}(nP)$  and  $h_b(n'P)$ , where the coupling constants take values in units of  $\text{GeV}^{-1/2}$ .

	$J = 0$	$J = 1$	$J = 2$	Units
$\chi_{bJ}(3P) \rightarrow h_b(2P) \gamma$	0.3	1.8	1.4	$(g_1' g_1'')^2 \text{ keV}$
$h_b(3P) \rightarrow \chi_{bJ}(2P) \gamma$	0.3	2.2	1.6	$(g_1' g_1'')^2 \text{ keV}$
$\chi_{bJ}(3P) \rightarrow h_b(1P) \gamma$	4.9	13.4	11.9	$(g_1 g_1'')^2 \text{ keV}$
$h_b(3P) \rightarrow \chi_{bJ}(1P) \gamma$	3.3	15.8	15.4	$(g_1 g_1'')^2 \text{ keV}$
$\chi_{bJ}(2P) \rightarrow h_b(1P) \gamma$	1.2	1.8	1.8	$(g_1 g_1')^2 \text{ keV}$
$h_b(2P) \rightarrow \chi_{bJ}(1P) \gamma$	0.7	2.0	2.5	$(g_1 g_1')^2 \text{ keV}$

quark electric charge (for a bottom quark,  $Q' = -1/3$ ), and  $m_Q$  is the mass of the heavy quark.

We specify the intermediate mesons in the list  $[m_1, m_2, m_3]$ , as denoted in Fig. 1. All the possible loops with the intermediate pseudoscalar and vector bottomed mesons are listed in Table 1 for the corresponding transitions. The pertinent transition amplitudes are given in Appendix A. From these amplitudes, one clearly sees two sources of spin symmetry breaking: the terms from the bottom quark magnetic moment are explicitly proportional to  $1/m_b$ , and the sum of  $\beta$ -terms in each amplitude vanishes if the vector and pseudoscalar bottom mesons are taken to be degenerate.<sup>1</sup>

The loops involved here are convergent, which means that the coupled-channel effects for the processes of interest are dominated by long-distance physics described in our NREFT. We do not need to introduce a counterterm here. The situation is different for the case of E1 transitions. The loop integrals involved there are divergent, and thus the contact term considered in Ref. [26] also serves as a counterterm and is necessary for renormalization.

Using the masses of the mesons given by the Particle Data Group [40], it is easy to get numerical results for the partial decay widths. As for the masses of the  $3P$  bottomonia, we choose the quark model values from Ref. [6], which were obtained based on the measured  $\chi_{bJ}(3P)$  mass by the LHCb Collaboration [41] with the predicted multiplet mass splittings, i.e.  $M_{h_b(3P)} = 10.519 \text{ GeV}$ ,  $M_{\chi_{b0}(3P)} = 10.500 \text{ GeV}$ ,  $M_{\chi_{b1}(3P)} = 10.518 \text{ GeV}$  and  $M_{\chi_{b2}(3P)} = 10.528 \text{ GeV}$ . These masses are very close to the ones in Ref. [7], where the coupled-channel effects are taken into account in a non-relativistic quark model. We also take  $\beta = 1/276 \text{ MeV}^{-1}$  [42], and  $m_b = 4.9 \text{ GeV}$ .

The decay amplitudes are proportional to the product squared of the coupling constants of the bottom and anti-bottom mesons to the  $1P$ ,  $2P$  and  $3P$  bottomonia, denoted as  $g_1$ ,  $g_1'$  and  $g_1''$ , respectively. As the mass of the  $\chi_{bJ}(1P, 2P, 3P)$  and  $h_b(1P, 2P, 3P)$  are below the bottom and anti-bottom meson threshold, the coupling constants cannot be measured directly. Here, we show the decay width of the hindered M1 transitions between two  $P$ -wave bottomonia in units of the coupling constants in the Table 2. The

**Table 3**

Comparison of the ratios of the decay widths for the  $2P$  to  $1P$  bottomonia with the ones from the RQM [6].

	$J = 0$		$J = 1$		$J = 2$	
	Ours	RQM	Ours	RQM	Ours	RQM
$\frac{\Gamma_{h_b(2P) \rightarrow \chi_{bJ}(1P) \gamma}}{\Gamma_{\chi_{bJ}(2P) \rightarrow h_b(1P) \gamma}}$	0.59	0.03	1.1	0.5	1.4	9.2

unknown parameters will get canceled if we calculate ratios of the decay widths which are proportional to the same product squared of coupling constants. Furthermore, we also expect that these ratios are less sensitive to the two-loop diagrams in Fig. 2 as the numerator and denominator in the ratio, being related to each other via spin symmetry, would get a similar correction. The ratios in our calculation can be easily obtained from Table 2. In order to show that the coupled-channel effects lead to very different values for some of these ratios, we show a comparison of ratios for selected decay widths of the hindered M1 transitions between the  $2P$  to  $1P$  bottomonia with those obtained in the quenched quark model of Ref. [6] in Table 3. These predictions can be tested in the future from experiments or lattice QCD calculations. In fact, radiative transitions of  $S$ -wave bottomonia, including the hindered M1 ones, have been studied by using lattice QCD [32,33,35]. As suggested in Ref. [28], one can check the coupled-channel effects directly in lattice QCD by comparing results in full and quenched calculations – the former includes the coupled-channel effects intrinsically while the latter does not.

As mentioned in Ref. [6], the numerical results of these hindered transitions in the quark model are very sensitive to relativistic corrections (these transitions do not vanish only when relativistic corrections are accounted for in quenched quark model). Nevertheless, they are tiny because the M1 transitions break heavy quark spin symmetry as well, and are in the ballpark of sub-eV to eV in Ref. [6]. If the partial widths really take such small values, an experimental observation of the bottomonium hindered M1 transitions would be impossible in the foreseeable future. In turn, this means that once such transitions are observed, the mechanism would be different from that in the quenched quark model, and would be caused by coupled-channel effects. Then, the measured partial widths can be used to estimate the involved coupling constants.

Unfortunately, the values of the coupling constants  $g_1$ ,  $g_1'$  and  $g_1''$  cannot be estimated reliably. If one takes the model estimate made in Ref. [43],<sup>2</sup>  $g_1 = -2\sqrt{m_{\chi_{b0}}/3}/f_{\chi_{b0}}$  and uses the value  $f_{\chi_{b0}} \approx 175 \text{ MeV}$  from a QCD sum rule calculation [45], then one gets  $g_1 \sim -20 \text{ GeV}^{-1/2}$ . This value is so large that if the  $\chi_{b0}$  is located only 1 MeV above the  $B^0 \bar{B}^0$  threshold it would have a huge width of 21 GeV. However, the quark model predictions for the open-bottom partial decay widths of the  $4P$  bottomonia leads to  $|g_1(4P)| \sim 0.2 \text{ GeV}^{-1/2}$  (the one for the  $5P$  states is slightly smaller), which, although it is for the  $4P$  states, is two orders of magnitude smaller than that from the former estimate. In Ref. [28], the product of the coupling constants  $(g_1 g_1')^2$  is estimated to be of order  $\mathcal{O}(10 \text{ GeV}^{-2})$  in the charm sector, where the difference between the model estimate for  $g_1$  [43] and the extracted value from quark model predictions of the  $2P$  charmonium decay widths is much smaller. If we naively take the same estimate here, despite that there is no simple flavor symmetry between charmonia and bottomonia, then the partial decay widths of  $\mathcal{O}(1 \sim 10^2) \text{ keV}$  could be large enough for a possible measurement in the future.

<sup>1</sup> For Eqs. (7), (8), (10), (11) given in Appendix A, this point is apparent, for Eqs. (9), (12), one can see this after taking the absolute value squared of the amplitude and summing up the polarizations.

<sup>2</sup> Here we have replaced the charmonium quantities by the corresponding bottomonium ones, and there is a factor of 2 difference for  $g_1$  in the definition of the Lagrangian in (5) and that in Ref. [43].

In principle, we can also calculate the decay widths for the isospin breaking transitions between the  $\chi_{bJ}(nP)$  states with the emission of one pion. They would be proportional to the same combination of unknown coupling constants. The charmonium analogues from the coupled-channel effects have been analyzed in details in Ref. [24]. However, we refrain from such a calculation because the isospin breaking between the charged and neutral bottom mesons is one order of magnitude smaller than that in the charmed sector because of the destructive interference between the contributions from the up and down quark mass difference and the electromagnetic effect [46].

In summary, we studied the hindered M1 transitions between two  $P$ -wave bottomonia,  $\chi_b(nP)$  and  $h_b(n'P)$  ( $n \neq n'$ ) assuming the mechanism is dominated by coupled-channel effects. Because of the suppression from heavy quark spin breaking and small relativistic corrections, such transitions have tiny partial widths from sub-eV to eV in quark model. In the mechanism underlying coupled-channel effects, the breaking of heavy quark spin symmetry can come from the different masses of bottom mesons within the same spin multiplet, and the problem of tiny matrix elements for transitions between bottomonia of different principal quantum numbers in the quark model does not exist as well. Therefore, it is natural to expect that the coupled-channel effects lead to much larger widths for such transitions than those predicted in the quark model. A future observation of such transitions at, e.g., Belle-II [29] may be regarded as a clear signal of the coupled-channel effects, and the measured widths could then be used to extract a rough value of the product of the so-far unknown coupling constants, e.g.  $g_1 g'_1$ . Such information would be useful for other transitions where intermediate bottom mesons play an important role, such as the decays of the  $Z_b(10610)$  and  $Z_b(10650)$  into  $h_b \pi$  and  $h_b(2P) \pi$ .

At last, we want to emphasize again that the coupled-channel effects in heavy quarkonium transitions can be checked directly in lattice QCD by comparing results from quenched and fully dynamical simulations as we already suggested in Ref. [28]. A better understanding of coupled-channel effects would lead to new insights into the dynamics of heavy quarkonia.

## Acknowledgements

We would like to thank Roberto Mussa for discussions and encouraging us to perform this study during the 2nd B2TiP Workshop. Two of the authors (UGM, ZY) gratefully acknowledge the hospitality at the ITP where this work was performed. This work is supported in part by the DFG and the NSFC through funds provided to the Sino-German CRC 110 “Symmetries and the Emergence of Structure in QCD” (NSFC Grant No. 11261130311), by the Thousand Talents Plan for Young Professionals, and by the Chinese Academy of Sciences President’s International Fellowship Initiative (Grant No. 2015VMA076).

## Appendix A. Decay amplitudes

The decay amplitude for each diagram is the sum of all possible triangle diagrams, and each diagram can be expressed in terms of convergent scalar three-point loop functions [24]

$$\begin{aligned} I(m_1, m_2, m_3) &= i \int \frac{d^4 l}{(2\pi)^4} \frac{1}{(l^2 - m_1^2 + i\epsilon) [(P-l)^2 - m_2^2 + i\epsilon] [(l-q)^2 - m_3^2 + i\epsilon]} \\ &= \frac{\mu_{12}\mu_{23}}{16\pi m_1 m_2 m_3} \frac{1}{\sqrt{a}} \left[ \tan^{-1} \left( \frac{c' - c}{2\sqrt{ac}} \right) + \tan^{-1} \left( \frac{2a + c - c'}{2\sqrt{a(c' - a)}} \right) \right], \quad (6) \end{aligned}$$

where  $a = (\mu_{23}/m_3)^2 \bar{q}^2$ ,  $c = 2\mu_{12}b_{12}$ ,  $c' = 2\mu_{23}b_{23} + (\mu_{23}/m_3)\bar{q}^2$ ,  $\mu_{ij} = m_i m_j / (m_i + m_j)$ ,  $b_{12} = m_1 + m_2 - M$  and  $b_{23} = m_2 + m_3 +$

$q^0 - M$ . In the loop function,  $P$  and  $q$  are the momenta of the initial bottomonium and the photon, respectively, and  $m_i$  ( $i = 1, 2, 3$ ) are the mass of the intermediate mesons. In the deriving of Eq. (6), the nonrelativistic approximation has been adopted.

The pertinent amplitudes for the decays are listed here:

$$\begin{aligned} \mathcal{M}_{\chi_{b0} \rightarrow \gamma h_b} &= -\frac{2iegg'}{\sqrt{3}} q^i \varepsilon^j(\gamma) \varepsilon_{ijk} \varepsilon^k(h_b) \\ &\times \sum_{a=u,d,s} \left\{ 2 \left( \beta Q_a + \frac{1}{3m_b} \right) I(B_a^*, \bar{B}_a^*, B_a^*) \right. \\ &\left. + \left( \beta Q_a - \frac{1}{3m_b} \right) [I(B_a^*, \bar{B}_a^*, B_a) - 3I(B_a, \bar{B}_a, B_a^*)] \right\}, \quad (7) \end{aligned}$$

$$\begin{aligned} \mathcal{M}_{\chi_{b1} \rightarrow \gamma h_b} &= 2i\sqrt{2}egg' [\vec{q} \cdot \vec{\varepsilon}(\chi_{b1}) \vec{\varepsilon}(\gamma) \cdot \vec{\varepsilon}(h_b) - \vec{q} \cdot \vec{\varepsilon}(h_b) \vec{\varepsilon}(\gamma) \cdot \vec{\varepsilon}(\chi_{b1})] \\ &\times \sum_{a=u,d,s} \left[ \left( \beta Q_a + \frac{1}{3m_b} \right) I(B_a^*, \bar{B}_a^*, B_a^*) \right. \\ &\left. - \left( \beta Q_a - \frac{1}{3m_b} \right) I(B_a, \bar{B}_a, B_a^*) \right], \quad (8) \end{aligned}$$

$$\begin{aligned} \mathcal{M}_{\chi_{b2} \rightarrow \gamma h_b} &= 4iegg' \varepsilon_{ijk} \varepsilon^{kl}(\chi_{b2}) \\ &\times \sum_{a=u,d,s} \left\{ -q^i \varepsilon^j(\gamma) \varepsilon^l(h_b) \left( \beta Q_a - \frac{1}{3m_b} \right) I(B_a^*, \bar{B}_a^*, B_a) \right. \\ &\left. + \varepsilon^i(h_b) [q^l \varepsilon^j(\gamma) - q^j \varepsilon^l(\gamma)] \right. \\ &\left. \times \left( \beta Q_a + \frac{1}{3m_b} \right) I(B_a^*, \bar{B}_a^*, B_a^*) \right\}, \quad (9) \end{aligned}$$

$$\begin{aligned} \mathcal{M}_{h_b \rightarrow \gamma \chi_{b0}} &= -\frac{2iegg'}{\sqrt{3}} q^i \varepsilon^j(\gamma) \varepsilon^k(h_b) \varepsilon_{ijk} \\ &\times \sum_{a=u,d,s} \left\{ 2 \left( \beta Q_a + \frac{1}{3m_b} \right) I(B_a^*, \bar{B}_a^*, B_a^*) \right. \\ &\left. + \left( \beta Q_a - \frac{1}{3m_b} \right) [I(B_a, \bar{B}_a^*, B_a^*) - 3I(B_a^*, \bar{B}_a, B_a)] \right\}, \quad (10) \end{aligned}$$

$$\begin{aligned} \mathcal{M}_{h_b \rightarrow \gamma \chi_{b1}} &= 2i\sqrt{2}egg' [\vec{q} \cdot \vec{\varepsilon}(\chi_{b1}) \vec{\varepsilon}(\gamma) \cdot \vec{\varepsilon}(h_b) - \vec{q} \cdot \vec{\varepsilon}(h_b) \vec{\varepsilon}(\gamma) \cdot \vec{\varepsilon}(\chi_{b1})] \\ &\times \sum_{a=u,d,s} \left[ \left( \beta Q_a + \frac{1}{3m_b} \right) I(B_a^*, \bar{B}_a^*, B_a^*) \right. \\ &\left. - \left( \beta Q_a - \frac{1}{3m_b} \right) I(B_a^*, \bar{B}_a^*, B_a) \right], \quad (11) \end{aligned}$$

$$\begin{aligned} \mathcal{M}_{h_b \rightarrow \gamma \chi_{b2}} &= 4iegg' \varepsilon_{ijk} \varepsilon^{kl}(\chi_{b2}) \\ &\times \sum_{a=u,d,s} \left\{ -q^i \varepsilon^j(\gamma) \varepsilon^l(h_b) \left( \beta Q_a - \frac{1}{3m_b} \right) I(B_a, \bar{B}_a^*, B_a^*) \right. \\ &\left. + \varepsilon^i(h_b) [q^l \varepsilon^j(\gamma) - q^j \varepsilon^l(\gamma)] \left( \beta Q_a + \frac{1}{3m_b} \right) I(B_a^*, \bar{B}_a^*, B_a^*) \right\}, \quad (12) \end{aligned}$$

where the initial bottomonium should be understood to be of higher excitation than the final one,  $\varepsilon^i(\gamma)$ ,  $\varepsilon^i(h_b)$  and  $\varepsilon^i(\chi_{b1})$  are



the polarization vectors for the photon,  $h_b$  and  $\chi_{b1}$ , respectively, and  $\varepsilon^{ij}(\chi_{b2})$  is the symmetric polarization tensor for the  $\chi_{b2}$ . One also needs to notice that a factor  $\sqrt{M_i M_f}$ , with  $M_{i,f}$  denoting the masses of the initial and final bottomonia, should be multiplied to each of the amplitudes to account for the nonrelativistic normalizations of the heavy quarkonium fields (similar factors for the intermediate heavy mesons have been absorbed in the definition of the loop function).

## References

- [1] J.P. Lees, et al., BaBar Collaboration, Phys. Rev. D 84 (2011) 091101, arXiv:1102.4565 [hep-ex].
- [2] M.B. Voloshin, Sov. J. Nucl. Phys. 43 (1986) 1011; Yad. Fiz. 43 (1986) 1571.
- [3] S. Godfrey, J.L. Rosner, Phys. Rev. D 66 (2002) 014012, arXiv:hep-ph/0205255.
- [4] U. Tamponi, et al., Belle Collaboration, Phys. Rev. Lett. 115 (2015) 142001, arXiv:1506.08914 [hep-ex].
- [5] F.-K. Guo, C. Hanhart, U.-G. Meißner, Phys. Rev. Lett. 105 (2010) 162001, arXiv:1007.4682 [hep-ph].
- [6] S. Godfrey, K. Moats, Phys. Rev. D 92 (2015) 054034, arXiv:1507.00024 [hep-ph].
- [7] J.F. Liu, G.J. Ding, Eur. Phys. J. C 72 (2012) 1981, arXiv:1105.0855 [hep-ph].
- [8] E. Eichten, K. Gottfried, T. Kinoshita, K.D. Lane, T.M. Yan, Phys. Rev. D 21 (1980) 203.
- [9] K. Heikkilä, S. Ono, N.A. Törnqvist, Phys. Rev. D 29 (1984) 110; Erratum: Phys. Rev. D 29 (1984) 2136.
- [10] E.J. Eichten, K. Lane, C. Quigg, Phys. Rev. D 73 (2006) 014014; Erratum: Phys. Rev. D 73 (2006) 079903, arXiv:hep-ph/0511179.
- [11] M.R. Pennington, D.J. Wilson, Phys. Rev. D 76 (2007) 077502, arXiv:0704.3384 [hep-ph].
- [12] T. Barnes, E.S. Swanson, Phys. Rev. C 77 (2008) 055206, arXiv:0711.2080 [hep-ph].
- [13] B.Q. Li, C. Meng, K.T. Chao, Phys. Rev. D 80 (2009) 014012, arXiv:0904.4068 [hep-ph].
- [14] I.V. Danilkin, Y.A. Simonov, Phys. Rev. D 81 (2010) 074027, arXiv:0907.1088 [hep-ph].
- [15] J. Ferretti, G. Galata, E. Santopinto, A. Vassallo, Phys. Rev. C 86 (2012) 015204.
- [16] Z.Y. Zhou, Z. Xiao, Eur. Phys. J. A 50 (2014) 165, arXiv:1309.1949 [hep-ph].
- [17] H.J. Lipkin, S.F. Tuan, Phys. Lett. B 206 (1988) 349.
- [18] P. Moxhay, Phys. Rev. D 39 (1989) 3497.
- [19] H.Y. Zhou, Y.P. Kuang, Phys. Rev. D 44 (1991) 756.
- [20] C. Meng, K.T. Chao, Phys. Rev. D 77 (2008) 074003, arXiv:0712.3595 [hep-ph].
- [21] C. Meng, K.T. Chao, Phys. Rev. D 78 (2008) 074001, arXiv:0806.3259 [hep-ph].
- [22] Y.A. Simonov, A.I. Veselov, Phys. Rev. D 79 (2009) 034024, arXiv:0804.4635 [hep-ph].
- [23] F.-K. Guo, C. Hanhart, U.-G. Meißner, Phys. Rev. Lett. 103 (2009) 082003; Erratum: Phys. Rev. Lett. 104 (2010) 109901, arXiv:0907.0521 [hep-ph].
- [24] F.-K. Guo, C. Hanhart, G. Li, U.-G. Meißner, Q. Zhao, Phys. Rev. D 83 (2011) 034013, arXiv:1008.3632 [hep-ph].
- [25] G. Li, Q. Zhao, Phys. Rev. D 84 (2011) 074005, arXiv:1107.2037 [hep-ph].
- [26] T. Mehen, D.L. Yang, Phys. Rev. D 85 (2012) 014002, arXiv:1111.3884 [hep-ph].
- [27] D.Y. Chen, X. Liu, X.Q. Li, Eur. Phys. J. C 71 (2011) 1808, arXiv:1109.1406 [hep-ph].
- [28] F.-K. Guo, U.-G. Meißner, Phys. Rev. Lett. 108 (2012) 112002, arXiv:1111.1151 [hep-ph].
- [29] R. Mussa, Talk given at the 2nd B2TiP Workshop, 27–29 April 2015, Krakow.
- [30] N. Brambilla, Y. Jia, A. Vairo, Phys. Rev. D 73 (2006) 054005, arXiv:hep-ph/0512369.
- [31] A. Pineda, J. Segovia, Phys. Rev. D 87 (7) (2013) 074024, arXiv:1302.3528 [hep-ph].
- [32] R. Lewis, R.M. Woloshyn, Phys. Rev. D 84 (2011) 094501, arXiv:1108.1137 [hep-lat].
- [33] R. Lewis, R.M. Woloshyn, Phys. Rev. D 86 (2012) 057501, arXiv:1207.3825 [hep-lat].
- [34] D. Bečirević, M. Kruse, F. Sanfilippo, J. High Energy Phys. 1505 (2015) 014, arXiv:1411.6426 [hep-lat].
- [35] C. Hughes, R.J. Dowdall, C.T.H. Davies, R.R. Horgan, G. von Hippel, M. Wingate, Phys. Rev. D 92 (2015) 094501, arXiv:1508.01694 [hep-lat].
- [36] F.-K. Guo, C. Hanhart, G. Li, U.-G. Meißner, Q. Zhao, Phys. Rev. D 82 (2010) 034025, arXiv:1002.2712 [hep-ph].
- [37] W. Detmold, C.-J.D. Lin, S. Meinel, Phys. Rev. Lett. 108 (2012) 172003, arXiv:1109.2480 [hep-lat].
- [38] F. Bernardoni, et al., ALPHA Collaboration, Phys. Lett. B 740 (2015) 278, arXiv:1404.6951 [hep-lat].
- [39] J.M. Flynn, et al., RBC and UKQCD Collaborations, Phys. Rev. D 93 (2016) 014510, arXiv:1506.06413 [hep-lat].
- [40] K.A. Olive, et al., Particle Data Group, Chin. Phys. C 38 (2014) 090001 and the 2015 update.
- [41] R. Aaij, et al., LHCb Collaboration, J. High Energy Phys. 1410 (2014) 88, arXiv:1409.1408 [hep-ex].
- [42] J. Hu, T. Mehen, Phys. Rev. D 73 (2006) 054003, arXiv:hep-ph/0511321.
- [43] P. Colangelo, F. De Fazio, T.N. Pham, Phys. Rev. D 69 (2004) 054023, arXiv:hep-ph/0310084.
- [44] J.F. Amundson, C.G. Boyd, E.E. Jenkins, M.E. Luke, A.V. Manohar, J.L. Rosner, M.J. Savage, M.B. Wise, Phys. Lett. B 296 (1992) 415, arXiv:hep-ph/9209241.
- [45] K. Azizi, H. Sundu, J.Y. Sungu, Eur. Phys. J. A 48 (2012) 108, arXiv:1207.5922 [hep-ph].
- [46] F.-K. Guo, C. Hanhart, U.-G. Meißner, J. High Energy Phys. 0809 (2008) 136, arXiv:0809.2359 [hep-ph].